Considering Actual Pipe Connections in Water Distribution Network Analysis

O. Giustolisi[1]

Abstract: The classical assumption of representing total demand along a pipe as two lumped withdrawals at its terminal nodes is hitherto common. It is a simplification of the network topology which is useful in order to drastically reduce the number of nodes during network simulation. Conversely, this simplification does not preserve energy balance equation of pipes and, for this reason, it is an approximation that could generate significant head loss errors. This paper presents a modification of the global gradient algorithm (GGA) which entails an enhancing of GGA (EGGA) permitting the effective introduction of the lumped nodal demands, without forfeiting correctness of energy balance, by means of a pipe hydraulic resistance correction. The robustness and convergence properties of the algorithm are compared with those of the classical GGA. Furthermore, the effectiveness of EGGA is demonstrated by computing the network pressure status under different configurations of the connections along the pipes of a test network.

DOI: 10.1061/(ASCE)HY.1943-7900.0000266

CE Database subject headings: Water distribution systems; Network analysis; Simulation; Algorithms; Water pipelines; Pipe networks.

Author keywords: Water distribution system; Network analysis; Simulation; Algorithms; Water pipelines; Pipe networks.

Introduction

The applications of local linearization methods (Cross 1936) and global linearization techniques characterized by the simultaneous solution of all the equations of the network analysis problem (Collins et al. 1978) are the two most important moments of existing studies on developing efficient network simulation algorithms (i.e., in terms of rapid convergence and robustness). The most comprehensive approach to global linearization techniques was set out by Collins et al. (1978) who defined the "content" and "cocontent" models. Different approaches to a global linearization technique are treated in the literature: Newton-Raphson global gradient algorithm (GGA) (Todini 1979; Todini and Pilati 1988); two similar approaches named Hybrid Method (Hamam and Brammeler 1971; Carpentier et al. 1987) and Newton Loop-Node Method (Osiadacz 1987); the Linear Theory Algorithm (Wood and Charles 1972; Isaacs and Mills 1980; Wood and Rayes 1981); the Newton-Raphson Loop Algorithm (an extension of the Cross method where loop equations are solved at the same time) (Epp and Fowler 1970; Kesavan and Chandrashekar 1972); and the Newton-Raphson Head Algorithm (Martin and Peters 1963; Shamir and Howard 1968). Among the aforementioned algorithms, the GGA (Todini 1979; Todini and Pilati 1988) was used to develop EPANET 2 (Rossman 2000), which has probably become the most widely used network simulation model in the world and which is also embedded in several commercial software packages.

All these algorithms require the iterative solution of a linear system of equations in order to reach the solution of the original mathematical system which is based on linear (due to mass balance) and nonlinear (due to energy balance) equations. However, the size of the linear system to be iteratively solved varies according to the method chosen as well as the information that has to be provided for formulating the linear system or identifying a first-attempt solution (i.e., to initialize the iterative process).

In all the previously discussed and available methods, actual water demands are generally represented as nodal withdrawals, although they are inevitably distributed along the pipes throughout connections to the properties. Such a simplification of nodal withdrawals was mainly justified by the lack of detailed and reliable knowledge about the position and number of actual connections. However, information, data and maps needed to analyze the water distribution networks (WDN) are today available and the use of information technology and geographical information system is becoming common in water industry in order to map systems and support management. In particular, the exact location of demands (e.g., the number and position of connections to the properties along mains of WDNs) permit a more detailed analysis of the hydraulic system. This aim could be potentially achieved by adding one node for each connection point, but this would drastically increase the complexity of the topological representation of the network model. Thus, the simplification of real demands as two lumped withdrawals at pipe terminal nodes is vital for maintaining acceptable computational times and for numerical reason related to the iterative solution of a linear system of equations whose size (e.g., in GGA) is the number of nodes of the topological representation. Unfortunately, the assumption of two equal lumped withdrawals (commonly one-half of the total pipe demand each) does not preserve the energy balance equation of pipes and significant head loss errors could affect the network analysis. This fact has been recently demonstrated by Giustolisi

[1]Professor, Dept. of Civil and Environmental Engineering, Engineering Faculty of Taranto, Technical Univ. of Bari, via E. Turismo 8 74100 Taranto, Italy. E-mail: o.giustolisi@poliba.it

Note. This manuscript was submitted on November 12, 2008; approved on April 25, 2010; published online on April 28, 2010. Discussion period open until April 1, 2011; separate discussions must be submitted for individual papers. This paper is part of the ***Journal of Hydraulic Engineering***, Vol. 136, No. 11, November 1, 2010. ©ASCE, ISSN 0733-9429/2010/11-889–900/$25.00.

and Todini (2009). They used the simple assumption of uniformly distributed demand along pipes and used the uniform function to model the demand pattern. It is worth noting that the results obtained in Giustolisi and Todini (2009) using such a classical "average" assumption are conceptually valid also for different shapes of distributed demands along a pipe (Hamberg and Shamir 1988). Furthermore, the assumption of uniform function for distributed demand along pipes is a lower bound for those errors, as will be demonstrated in the paper.

Thus, this paper will present the extension of GGA (i.e., EGGA) permitting the effective introduction of the lumped nodal demands while preserving the energy balance by means of a pipe hydraulic resistance correction. Although the strategy is proposed herein as a modification of GGA, other standard hydraulic commercial software [e.g., a specific numerical minimization of the Content energy function (Carpentier et al. 1987; Piller 1995)] that relies on other algorithms can benefit from the presented advancement as well. Finally, the simplification reported here should be not confused with network skeletonization in the sense of model simplification (Anderson and Al-Jamal 1995) through linearization around a given working point by eliminating all redundant nodes through the Gauss-Jordan elimination technique (Ulanicki et al. 1996). In fact, the scope here is to account for general shapes of demand distribution along pipes as reported in Hamberg and Shamir (1988) by considering the adjustment of the network simulation model (GGA, for example) in order to continue using the schematization of the demands as two concentrated water withdrawals at the terminal nodes of pipes while preserving both energy and mass balance equations.

It is noteworthy that EGGA has two complementary uses:

1. A more precise modeling of the network (i.e., of demand pattern along mains) without any approximation on energy balance and without increasing the number of nodes (i.e., the topological representation of the model); and
2. To simplify the existing network topologies with respect to serial nodes (delivering demand) and trunks without any approximation on energy balance.

Furthermore, EGGA has numerical advantages, as reported and discussed thought paper, which are a practical advantage, independently on improved accuracy of the analysis or model topology reduction.

Network Simulation Model

The demand-driven simulation of a network of n_p pipes with unknown flows/discharges, n_n nodes with unknown heads (internal nodes), and n_0 nodes with known heads (tank levels, for example) can be formulated in the following partly non-linear and partly linear system based on energy and mass balance equations:

$$\mathbf{A}_{pp}\mathbf{Q}_p + \mathbf{A}_{pn}\mathbf{H}_n = -\mathbf{A}_{p0}\mathbf{H}_0$$

$$\mathbf{A}_{np}\mathbf{Q}_p = \mathbf{d}_n \tag{1}$$

where $\mathbf{Q}_p=[n_p,1]$ column vector of unknown pipe flow rates; $\mathbf{H}_n=[n_n,1]$ column vector of unknown nodal heads; $\mathbf{H}_0=[n_0,1]$ column vector of known nodal heads; $\mathbf{d}_n=[n_n,1]$ column vector of demands lumped in the nodes driving the simulation; $\mathbf{A}_{pn}=\mathbf{A}_{np}^T$ and $\mathbf{A}_{p0}$=topological incidence submatrices of size $[n_p,n_n]$ and $[n_p,n_0]$, respectively, derived from the general topological matrix $\bar{\mathbf{A}}_{pn}=[\mathbf{A}_{pn}|\mathbf{A}_{p0}]$ of size $[n_p,n_n+n_0]$, as defined in Todini and Pilati (1988). Furthermore, in the first equation of the system (1) $\mathbf{A}_{pp}\mathbf{Q}_p=[n_p,1]$ column vector of pipe head loss whose elements are, according to Darcy-Weisbach formulation

$$E_k = \frac{8f_k(\mathrm{Re},\mathrm{Ke})}{g\pi^2 D_k^5}Q_k|Q_k|L_k = R_k(\mathrm{Re},\mathrm{Ke},D,L)Q_k|Q_k| \tag{2}$$

where k=subscript of pipe variables; f_k=pipe friction factor dependent on Re=Reynolds number and the Ke=equivalent roughness; D_k=pipe internal diameter; g=gravitational acceleration constant; Q_k=pipe flow rate; and L_k=pipe length. Thus, R_k is the pipe hydraulic resistance that is a function of Re (i.e., Q_k), Ke, pipe diameter D, and pipe length L. Eq. (2), the Darcy-Weisbach formulation of head losses, holds for laminar, rough turbulent and fully rough turbulent flow regimes.

In technical practice, Eq. (2) is very often substituted by

$$E_k = R_k(\mathrm{Ke},D,L)Q_k|Q_k|^{n-1} = R_{k,\infty}Q_k|Q_k|^{n-1} \tag{3}$$

where $R_{k,\infty}$ is not dependent on flow regime (i.e., Q_k) and is, therefore, constant during network simulations, while n =exponent dependent on adopted head loss relationship (i.e., 1.852 for the Hazen-Williams and 2 for the Darcy-Weisbach fully rough turbulent flow).

In this paper, the formulation $R_kQ_k|Q_k|^{n-1}$ for the kth pipe head loss will be used with the following meaning:

- $n=2$ and $R_k=R_k(Q_k)$ for general Darcy-Weisbach formulation of pipe head losses;
- $n=2$ and $R_k=R_{k,\infty}$=const, for Darcy-Weisbach formulation of pipe head losses and fully rough turbulent flow assumption; and
- $n=1.852$ with $R_k=R_{k,\infty}$=const for Hazen-Williams formulation of pipe head losses.

EGGA Framework

In order to explain the enhanced GGA (EGGA) strategy, the water network model in Eq. (1) will be used as reference point. The network model (1) requires the boundary conditions $(\mathbf{R}_p;\mathbf{d}_n;\mathbf{H}_0)$, where $\mathbf{R}_p$=vector of pipe resistances, in order to compute the unknowns $(\mathbf{Q}_p;\mathbf{H}_n)$. In addition, that hydraulic model requires the topological representation of the network (i.e., $\bar{\mathbf{A}}_{pn}$). Considering Fig. 1, it is possible to identify two kinds of internal nodes: (1) nodes representing the exact location of demands which are internal to pipes as in Fig. 1(b); and (2) nodes joining more than two pipes (generally not delivering any demand in real networks) which are necessary to represent the connectivity among main pipes, as for Examples A and B in Fig. 1. Actually, the case (2) can be extended to nodes not joining pipes (they are the terminal nodes of branched parts) and it is to observe that the nodes joining two pipes and not delivering any demand can be removed by simply summing pipe resistances. It is obvious that the topological representation of the hydraulic system of Fig. 1(a) is parsimonious. It preserves the mass balance because the total demand P_k of the kth pipe is concentrated at its terminal nodes using the lumping coefficient α_k (commonly equal to 0.5), but the energy balance results forfeited (Giustolisi and Todini 2009). The topological representation of the hydraulic system of Fig. 1(b) is the most accurate in order to preserve the energy balance, but it requires the introduction of a number of nodes internal to the kth pipe equal to connection points. This strategy is not parsimonious with respect to the dimension of the topological representation of the network (i.e., $\bar{\mathbf{A}}_{pn}$ size) because it introduces nodes and trunks, whose variables are indicated by the subscripts j and i,

J. Hydraul. Eng., 2010, 136(11): 889-900

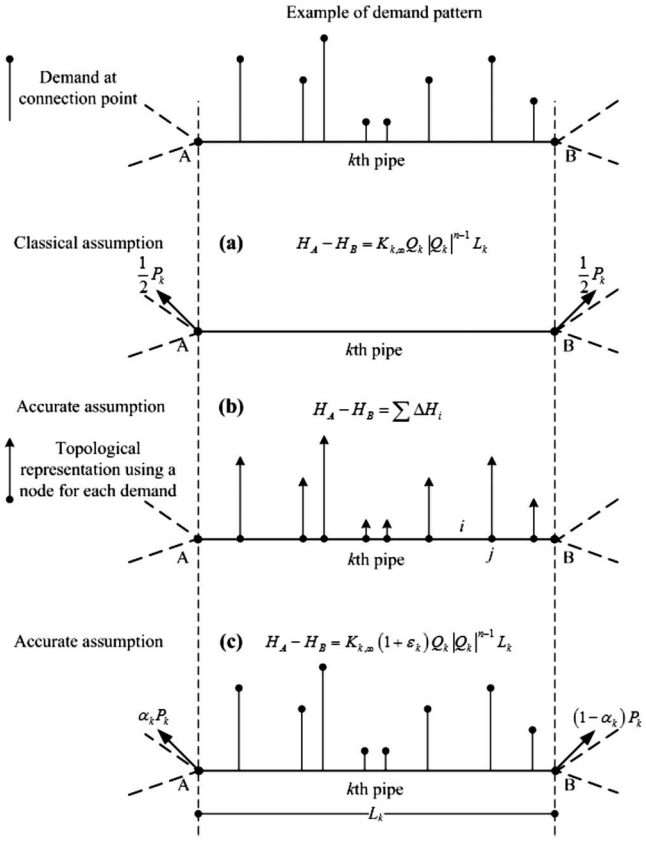

Fig. 1. Topological representation of network and EGGA strategy

respectively. They are designated as "inline nodes" and "inline trunks," respectively. Two main disadvantages of increasing the topology dimension are as follows: (1) size of the numerical problem associated with the iterative solution of a linear system within the network model rises and (2) computational efficiency and efficacy decreases e.g. for real-time analyses, optimal design and rehabilitation, etc., purposes. In order to maintain the same model accuracy of Fig. 1(b) (with respect to energy balance) without increasing the dimension of the topological representation of the hydraulic network, Giustolisi and Todini (2009) proposed the strategy reported in Fig. 1(c). They introduced the hydraulic resistance correction factor ε_k which can be easily formulated under the assumption of a uniform function to represent demand patterns.

This work will demonstrate that the strategy based on the hydraulic resistance correction factor ε_k is of general validity. In fact, it will be extended to the case of exact location of the actual demand connections without any assumption on flow regime and considering different unitary hydraulic resistances among the inline trunks (e.g. due to diameter change). The presence of valves and pumps will be considered in the formulation of the correction factor ε_k and the numerical properties of the strategy will be proved via numerical tests. Furthermore, regularization capability of the strategy with respect to simulation model algorithms will be discussed.

For the sake of clarity, it is important to emphasize that $\mathbf{d}_n$ of system (1) is obtained as sum of lumped demands (i.e., demands concentrated as water withdrawals at terminal nodes) of pipes originally joined at those nodes. It is computed in EGGA by

$$\mathbf{d}_n = \mathbf{\Lambda}_{np}\mathbf{P}_p \tag{4}$$

where $\mathbf{P}_p=[P_1,\ldots,P_k,\ldots,P_{np}]^{\mathrm{T}}$=pipe demand vector whose elements P_k=total demand distributed along each kth pipe. The matrix Λ_{np} is built from matrix A_{np} substituting into each kth column -1 and $+1$ the value α_k and $(1-\alpha_k)$, respectively. It is worth noting that sum of elements for each column of Λ_{np} is equal to the unit in order to preserve mass balance while concentrating P_k at terminal nodes. The case $\alpha_k=1/2$ corresponds to $\Lambda_{np}=|\mathrm{A}_{np}|/2$ (i.e., most common technical assumption). Consequently, Eq. (4) is a useful generalization for EGGA purposes. It is noteworthy that explicating the way $\mathbf{d}_n$ is formed from P_k by means of $\mathbf{\Lambda}_{np}$ helps in understanding the source of uncertainty of $\mathbf{d}_n$ itself. Furthermore, EGGA simplification of the topological representation of the hydraulic system by removing inline nodes is beneficial for managing demand uncertainty since they are integrated in P_k and then concentrated in a lower size vector $\mathbf{d}_n$.

EGGA Formulation

Starting from the energy balance equation corrected by the hydraulic resistance correction factor ε_k

$$E_k = R_{k,\infty}(1+\varepsilon_k)Q_k|Q_k|^{n-1} \tag{5}$$

the matrix $\mathbf{A}_{pp}$, whose diagonal elements are now $R_{k,\infty}(1+\varepsilon_k)|Q_k|^{n-1}$ can be rewritten as function of $\delta_k=Q_k/P_k$ which is a dimensionless parameter ratio of the simulation model pipe flow (Q_k) and total distributed demand (P_k) of the kth pipe considering Fig. 1(c). Hence

$$A_{pp}(k,k) = R_{k,\infty}(|\delta_k|^{n-1} + \varepsilon_k|\delta_k|^{n-1})P_k^{n-1} = R_{k,\infty}(|\delta_k|^{n-1} + zA_k)P_k^{n-1} \tag{6}$$

At the same time, the energy balance correction ΔE_k is

$$\Delta E_k = R_{k,\infty}\varepsilon_k Q_k|Q_k|^{n-1} = R_{k,\infty}\varepsilon_k\delta_k|\delta_k|^{n-1}P_k^n = R_{k,\infty}z_kP_k^n \tag{7}$$

and the elements of the diagonal matrix $\mathbf{D}_{pp}$, which are the derivatives of E_k with respect to Q_k are

$$D_{pp}(k,k) = \frac{dE_k}{dQ_k} = R_{k,\infty}\left(n|\delta_k|^{n-1} + \frac{dz_k}{d\delta_k}\right)P_k^{n-1}$$
$$= R_{k,\infty}(n|\delta_k|^{n-1} + zD_k)P_k^{n-1} \tag{8}$$

Thus, the relations between each pair of the four dimensionless correction factors $(\varepsilon_k, z_k, zA_k, zD_k)$ is

$$z_k = \varepsilon_k\delta_k|\delta_k|^{n-1} \quad zA_k = \frac{z_k}{\delta_k} \quad zD_k = \frac{dz_k}{d\delta_k} \tag{9}$$

Then, considering the solution of the system (1) given by Todini and Pilati (1988)

$$\mathbf{B}_{pp}^{\mathrm{iter}} = (\mathbf{D}_{pp}^{\mathrm{iter}})^{-1}\mathbf{A}_{pp}^{\mathrm{iter}}$$

$$\mathbf{F}_n^{\mathrm{iter}} = -\mathbf{A}_{np}(\mathbf{I}_{pp} - \mathbf{B}_{pp}^{\mathrm{iter}})\mathbf{Q}_p^{\mathrm{iter}} + \mathbf{d}_n + \mathbf{A}_{np}(\mathbf{D}_{pp}^{\mathrm{iter}})^{-1}(\mathbf{A}_{p0}\mathbf{H}_0)$$

$$\mathbf{H}_n^{\mathrm{iter+1}} = -(\mathbf{A}_{np}(\mathbf{D}_{pp}^{\mathrm{iter}})^{-1}\mathbf{A}_{pn})^{-1}\mathbf{F}_n^{\mathrm{iter}}$$

$$\mathbf{Q}_p^{\mathrm{iter+1}} = (\mathbf{I}_{pp} - \mathbf{B}_{pp}^{\mathrm{iter}})\mathbf{Q}_p^{\mathrm{iter}} - (\mathbf{D}_{pp}^{\mathrm{iter}})^{-1}(\mathbf{A}_{p0}\mathbf{H}_0 + \mathbf{A}_{pn}\mathbf{H}_n^{\mathrm{iter+1}}) \tag{10}$$

where iter=iteration counter used during the iterative solution; $\mathbf{F}_n$=vector of known terms of the linear system of equations to be iteratively solved; and $\mathbf{I}_{pp}$=identity matrix, it is necessary to achieve the diagonal elements of the matrix $\mathbf{B}_{pp}$, hence

J. Hydraul. Eng., 2010, 136(11): 889-900

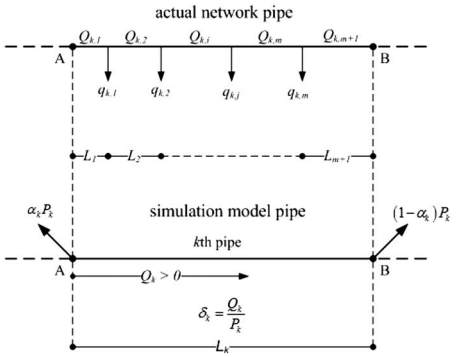

Fig. 2. Actual pipe connections and schematic representation in simulation model

$$\frac{A_{pp}(k,k)}{D_{pp}(k,k)} = \frac{|\delta_k|^{n-1} + zA_k}{n|\delta_k|^{n-1} + zD_k} = zB_k \tag{11}$$

In conclusion, the difference between GGA and EGGA is the way the matrices $\mathbf{A}_{pp}$, $\mathbf{B}_{pp}$, and $\mathbf{D}_{pp}$ are formed. In the following equations, the square brackets evidence the terms to be added to GGA in order to have EGGA:

$$A_{pp}(k,k) = R_{k,\infty}|Q_k|^{n-1} + [R_{k,\infty} z A_k P_k^{n-1}]$$

$$D_{pp}(k,k) = nR_{k,\infty}|Q_k|^{n-1} + [R_{k,\infty} z D_k P_k^{n-1}]$$

$$B_{pp}(k,k) = \frac{A_{pp}(k,k)}{D_{pp}(k,k)} = \frac{|Q_k|^{n-1} + [zA_k P_k^{n-1}]}{n|Q_k|^{n-1} + [zD_k P_k^{n-1}]} = zB_k \tag{12}$$

It is important to note that zD_k and zA_k tend to zero when δ_k tends to infinity (i.e., P_k is negligible with respect to Q_k) and the element zB_k of the diagonal matrix $\mathbf{B}_{pp}$ becomes equal to $1/n$ (i.e., 0.5 for $n=2$). Consequently, in such circumstance, EGGA coincides with GGA for the kth pipe.

Furthermore, it is worth noting that the assumption $R_{k,\infty}$ (i.e., a constant pipe hydraulic resistance) in Eq. (5) implies that the correction ε_k can account for the error due to the adoption of $f(\mathrm{Ke})$ instead of $f(\mathrm{Re},\mathrm{Ke})$. For example, considering the case of $P_k=0$, it easy to demonstrate that $\varepsilon_k = R_k/R_{k,\infty} - 1$. Finally, as example, the Appendix reports the values of the dimensionless factors obtained by Giustolisi and Todini (2009) using the uniform function to represent the demand pattern and $\alpha_k=0.5$.

General Head Loss Correction

The aim of this section is to calculate the hydraulic resistance correction factor ε_k for the most general condition of m_k connections along the kth pipe delivering the demands $q_{k,j}$, as reported in Fig. 2. Thus, the general formulation for total head loss considering pipe A-B

$$(H_A - H_B)_{\text{actual}} = K_{k,1} Q_{k,1} |Q_{k,1}|^{n-1} L_{k,1} + \sum_{i=1}^{m_k} K_{k,i+1} \left(Q_{k,1} - \sum_{j=1}^{i} q_{k,j} \right) \times \left| Q_{k,1} - \sum_{j=1}^{i} q_{k,j} \right|^{n-1} L_{k,i+1}$$

$$\text{where} \quad Q_{k,i} = Q_{k,1} - \sum_{j=1}^{i} q_{k,j} \tag{13}$$

where $Q_{k,i}$=flows of inline trunks; $q_{k,j}$=demands of the m_k connections (inline nodes) and $L_{k,i}$ and $K_{k,i}$=lengths and the unitary hydraulic resistances (possibly dependent on flow regime) of the m_k+1 inline trunks, respectively. Eq. (13) can be rewritten considering the dimensionless parameters

$$\kappa_{k,i} = \frac{K_{k,i}}{K_{k,\infty}} \quad \forall\, k \in [1,n_p],\ \forall\, i \in [1,m_k+1]$$

$$\lambda_{k,i} = \frac{L_{k,i}}{L_k} \quad \forall\, k \in [1,n_p],\ \forall\, i \in [1,m_k+1]$$

$$\pi_{k,i} = \frac{\sum_{j=1}^{i} q_{k,j}}{P_k}, \pi_{k,0} \triangleq 0 \quad \forall\, k \in [1,n_p],\ \forall\, i \in [0,m_k]$$

$$\delta_k + \alpha_k = \frac{Q_{k,1}}{P_k} \Leftrightarrow \delta_k = \frac{Q_k}{P_k} \quad \forall\, k \in [1,n_p] \tag{14}$$

where $K_{k,\infty}$=unitary hydraulic resistance of fully rough turbulent flow regime of the trunk $i=1$ which is conventionally attributed to the kth pipe. The last of Eq. (14) holds in order to preserve mass balance (i.e., $Q_{k,1}$ of the first inline trunk is equal to $Q_k+\alpha_k P_k$). This way Eq. (13) becomes

$$(H_A - H_B)_{\text{actual}} = K_{k,\infty} L_k \left(\sum_{i=0}^{m_k} \kappa_{k,i+1} (\delta_k + \alpha_k - \pi_{k,i}) |\delta_k + \alpha_k - \pi_{k,i}|^{n-1} \lambda_{k,i+1} \right) P_k^n \tag{15}$$

It is to be emphasized that the demand distribution along the kth pipe is not symmetric with respect to flow direction [i.e., the summation to compute $\pi_{k,i}$ depends on flow direction, see third of Eq. (14)]. Consequently, Eq. (15) has been written considering the positive flow direction. Furthermore, considering Eq. (5) and assuming $R_{k,\infty}=K_{k,\infty}L_k$ (i.e., pipe resistances in EGGA framework are conventionally obtained by the unitary hydraulic resistance of fully rough turbulent flow regime of the first inline trunk multiplied by the total pipe length), it is possible to write

$$(H_A - H_B)_{\text{EGGA}} = K_{k,\infty} L_k (1+\varepsilon_k) Q_k |Q_k|^{n-1} = K_{k,\infty} L_k (1+\varepsilon_k) \delta_k |\delta_k|^{n-1} P_k^n \tag{16}$$

The condition $(H_A-H_B)_{\text{actual}}=(H_A-H_B)_{\text{EGGA}}$ allows to preserve the energy balance in the simulation model (EGGA) with respect to the actual demand pattern. Thus, the correction factor is given by

$$\varepsilon_k = \frac{\sum_{i=0}^{m_k} \kappa_{k,i+1} (\delta_k + \alpha_k - \pi_{k,i}) |\delta_k + \alpha_k - \pi_{k,i}|^{n-1} \lambda_{k,i+1}}{\delta_k |\delta_k|^{n-1}} - 1 \tag{17}$$

Now, it is possible to obtain z_k, zD_k and zA_k from Eq. (9) and zB_k from Eq. (11).

In particular for zD_k it is possible to write

$$zD_k = \frac{dz_k}{d\delta_k} = \sum_{i=0}^{m_k} \left[\left(P_k \frac{d\kappa_{k,i+1}}{dQ_{k,i+1}} (\delta_k + \alpha_k - \pi_{k,i}) + n\kappa_{k,i+1} \right) |\delta_k + \alpha_k - \pi_{k,i}|^{n-1} \lambda_{k,i+1} \right] - n|\delta_k|^{n-1} \quad (18)$$

where the terms $d\kappa_{k,i}/dQ_{k,i}$ are null if the fully rough turbulent flow is assumed.

Now, ε_k, z_k, zD_k, and zA_k are generally dependent on δ_k, as found in Giustolisi and Todini (2009), see the Appendix (where the uniform function has been used as a surrogate of the uniformly distributed demands), but also on $\lambda_{k,i}$ and $\pi_{k,i}$, which are parameters related to demand distribution patterns; $\kappa_{k,i}$ and n, which are parameters related to flow regime; and α_k, which is the parameter related to the way the total pipe demand is lumped at pipe terminal nodes.

After all, it is important to note that α_k are not parameters to be calibrated because they are useful to lump the demand in the general case of non symmetric demand pattern (see later in the text). In addition, EGGA does not increase the number of unitary hydraulic resistances to be calibrated since, when it is used: to remove inline nodes, the values of unitary hydraulic resistances of inline trunks used to compute the correction factors (i.e., $\kappa_{k,i}$) are already existing in GGA (i.e., before topological simplification); to describe the demand pattern of mains (i.e., in its complementary way), unitary hydraulic resistances of inline trunks are constant and $\kappa_{k,i}=1$ holds.

In conclusion, in order to further generalize the correction factor ε_k, a pump installed in the trunk $i=p$ and a minor head loss in $i=v$ are hereby assumed. This way, assuming the following parameters:

$$G_k = \frac{D_{k,1}}{f_{k,\infty} L_k P_k^{n-2}}$$

$$\text{on} = [r_{k,p}(\delta_k + \alpha_k - \pi_{k,p}) \geq 0]$$

$$H_{k,p}^I = \text{on} \frac{\omega_{k,p}^2 H_{k,p}}{R_{k,\infty} P_k^n} \quad r_{k,p}^I = \text{on} \frac{\omega_{k,p}^{2-\gamma} |r_{k,p}|}{R_{k,\infty} P_k^{n-\gamma}} \quad (19)$$

the hydraulic resistance correction factor becomes

$$\varepsilon_k = \frac{\sum_{i=0}^{m_k} \kappa_{k,i+1} (\delta_k + \alpha_k - \pi_{k,i}) |\delta_k + \alpha_k - \pi_{k,i}|^{n-1} \lambda_{k,i+1}}{\delta_k |\delta_k|^{n-1}} + \frac{-\text{sign}(r_{k,p})(H_{k,p}^I - r_{k,p}^I |\delta_k + \alpha_k - \pi_{k,p}|^\gamma P_k^{\gamma-n})}{\delta_k |\delta_k|^{n-1}} + \frac{\frac{A_{k,1}^2}{A_{k,v}^2} K_{k,v}^{ml} G_k (\delta_k + \alpha_k - \pi_{k,v}) |\delta_k + \alpha_k - \pi_{k,v}|}{\delta_k |\delta_k|^{n-1}} - 1 \quad (20)$$

where $A_{k,i}$=internal cross sectional area of the ith inline trunk and $D_{k,1}$ and $f_{k,\infty}$=internal diameter and the friction factor (of fully rough turbulent flow) of the first inline trunk of the kth pipe, respectively. Furthermore, $\omega_{k,p}$, $H_{k,p}$, $r_{k,p}$, γ=pump speed factor and parameters of pump curve [for further details see EPANET 2 tutorial (Rossman 2000)]; $K_{k,v}^{ml}$=minor head loss coefficient and on=Boolean variable that accounts for the pump installation direction. The sign of $r_{k,p}$ is related to pump installation direction: a positive $r_{k,p}$ means that the installation of the pump is coherent with the positive direction assigned to flow in WDN model. Clearly, if the sign $r_{k,p}$ differs on actual flow, on<0, the pump does not work and it should be substituted by a closed valve assuming that pumps are always equipped with a nonreturn valve.

Finally, referring to Fig. 1 case (c), it is useful to emphasize that although the parsimonious topological representation of the hydraulic system has been used in EGGA, the internal nodal heads (inline nodes) and flows (inline trunks) can be easily computed from Eqs. (13) and (14). In fact, EGGA provides Q_k of the kth pipe and H_A, while α_k, P_k, $\pi_{k,i}$, $K_{k,i}$, and $\lambda_{k,i}$ are known and $Q_{k,1}$ of the first trunk is $Q_{k,1}=Q_k+\alpha_k P_k$.

Analysis of Multiple Uniformly Spaced Connection with Equal Demands

In order to study Eq. (17), $n=2$ (i.e., Darcy-Weisbach formulation for fully rough turbulent flow regime), $q_{k,j}$=const (i.e., a uniform distributed demand with m_k connections and $\pi_{k,i}=i/m_k$), $\lambda_{k,i}$ =const (i.e., $\lambda_{k,i}=1/(m_k+1)$), $\kappa_{k,i}=1$ and $\alpha_k=0.5$ (because of the symmetry of the demand pattern) have been assumed here. This way, Eqs. (9) and (17) can be rewritten as

$$\varepsilon_k = \frac{1}{m_k+1} \frac{\sum_{i=0}^{m_k} \left(\delta_k + \frac{1}{2} - \frac{i}{m_k} \right) \left| \delta_k + \frac{1}{2} - \frac{i}{m_k} \right|}{\delta_k |\delta_k|} - 1$$

$$z_k = \frac{1}{m_k+1} \sum_{i=0}^{m_k} \left(\delta_k + \frac{1}{2} - \frac{i}{m_k} \right) \left| \delta_k + \frac{1}{2} - \frac{i}{m_k} \right| - \delta_k |\delta_k| \quad (21)$$

The dimensionless factors ε_k and z_k have been plotted in Fig. 3 (together with zD_k and zB_k) for the cases $m=m_k=[1,2,4,8]$ along with the uniform function case used in Giustolisi and Todini (2009). The five curves of each subplot of Fig. 3 confirm that the figure of the dimensionless factors ε_k, z_k, zD_k, and zB_k is similar for all the five cases (uniform function plus uniform demand distribution varying m) because of the symmetric property of demand patterns. Thus, as for the case of uniform function (Giustolisi and Todini 2009), the correction ε_k is always positive causing the underestimation of the head losses in GGA, see Eq. (7). This fact leads to the overestimation of hydraulic resistance during hydraulic system calibration as demonstrated in Giustolisi and Todini (2009). Fig. 3 shows also that, for a given δ_k, the lowest correction ε_k for pipe energy balance occurs when the uniform function is used; consequently, the largest correction occurs for $m_k=1$. Furthermore, increasing m the curves $\varepsilon_k=\varepsilon_k(m)$ rapidly approach the curve of uniform function. Therefore, the uniform function is a lower bound of the correction ε_k (i.e., its use underestimates the correction with respect to m_k uniformly distributed connections) but increasing m_k the underestimation quickly decreases. Finally, the correction ε_k tends to zero increasing δ_k, independently on m_k, as expected from the previous findings using the uniform function. The subplot $z_k=z_k(m)$ of Fig. 3 further demonstrates that the pipe head losses are underestimated, see Eq. (7), considering that the values z_k are negative or positive for Q_k (i.e., δ_k) negative and positive, respectively. In addition the curves $z_k(m)$ as well z_k of the uniform function reach a constant value when $\delta_k=\pm 0.5$. The upper bounds of curves $z_k(m)$ in Fig. 3 further demonstrate that the case of one connection corresponds to the maximum energy balance error of classical GGA. Finally, the subplots of zD_k and zB_k of Fig. 3 evidence that those values are always finite ranging in [0 1] and [0.5 1], respectively. Reminding that zD_k is the derivative of z_k with respect to δ_k, its

J. Hydraul. Eng., 2010, 136(11): 889-900

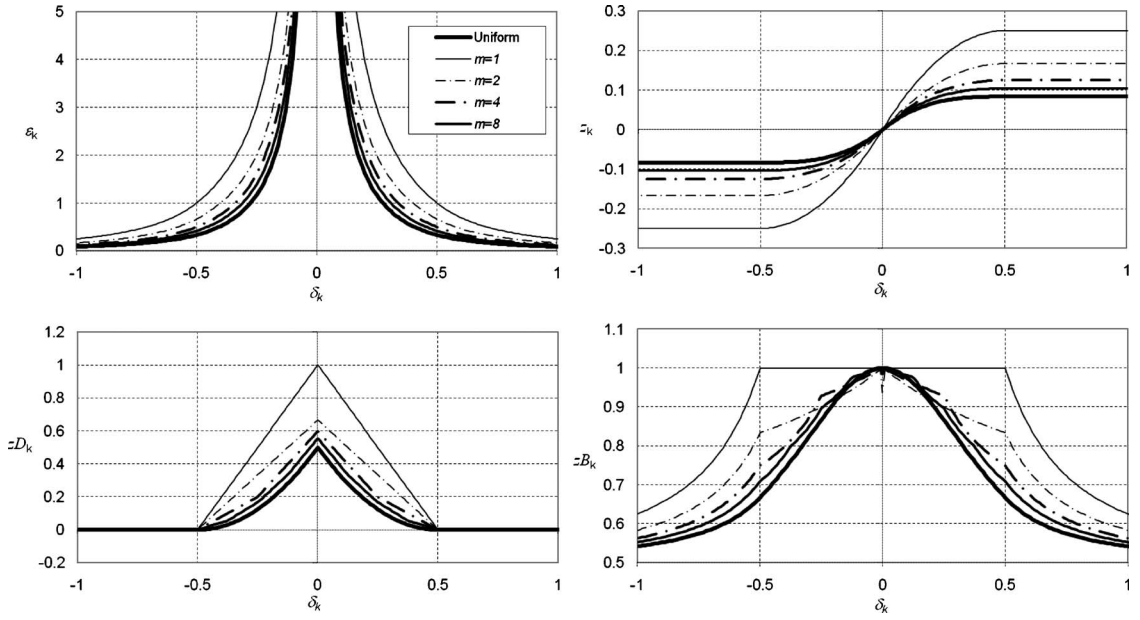

Fig. 3. Subplots of ε_k, z_k, zD_k, and zB_k as a function of δ_k considering uniform demand distribution

value is equal to zero when $\delta_k = \pm 0.5$ (consistently with top-right Fig. 3), while zB_k asymptotically tends to the value 0.5 as $|\delta_k|$ increases as already discussed with respect to Eq. (12).

Analysis of One Connection Pipe

Eqs. (9) and (17) are studied here using the case of one active connection only along the pipe ($m_k=1$) and once more assuming $n=2$ and $\kappa_{k,1}=1$. This is useful because the previous section demonstrates that the case of one active connection is the upper bound of the correction factor ε_k. Hence, Eqs. (9) and (17) can be rewritten as

$$\varepsilon_k = \frac{(\delta_k+\alpha_k)|\delta_k+\alpha_k|\lambda_{k,1}+(\delta_k+\alpha_k-1)|\delta_k+\alpha_k-1|(1-\lambda_{k,1})}{\delta_k|\delta_k|} - 1$$

$$z_k = (\delta_k+\alpha_k)|\delta_k+\alpha_k|\lambda_{k,1}+(\delta_k+\alpha_k-1)|\delta_k+\alpha_k-1|(1-\lambda_{k,1}) - \delta_k|\delta_k| \quad (22)$$

The dimensionless factors ε_k and z_k, have been plotted in Fig. 4 for the cases $\lambda_{k,1}=\{0.7, 0.9\}$ using $\alpha_k=0.5$ and two different values of α_k as will be clarified in the next section. In fact, both the curves for $\lambda_{k,1}=0.7$ and 0.9 demonstrate that assuming $\alpha_k=0.5$ the correction ε_k tends to minus infinity for $\delta_k=0^-$ and to plus infinity for $\delta_k=0^+$. The negative values of the correction are caused by the

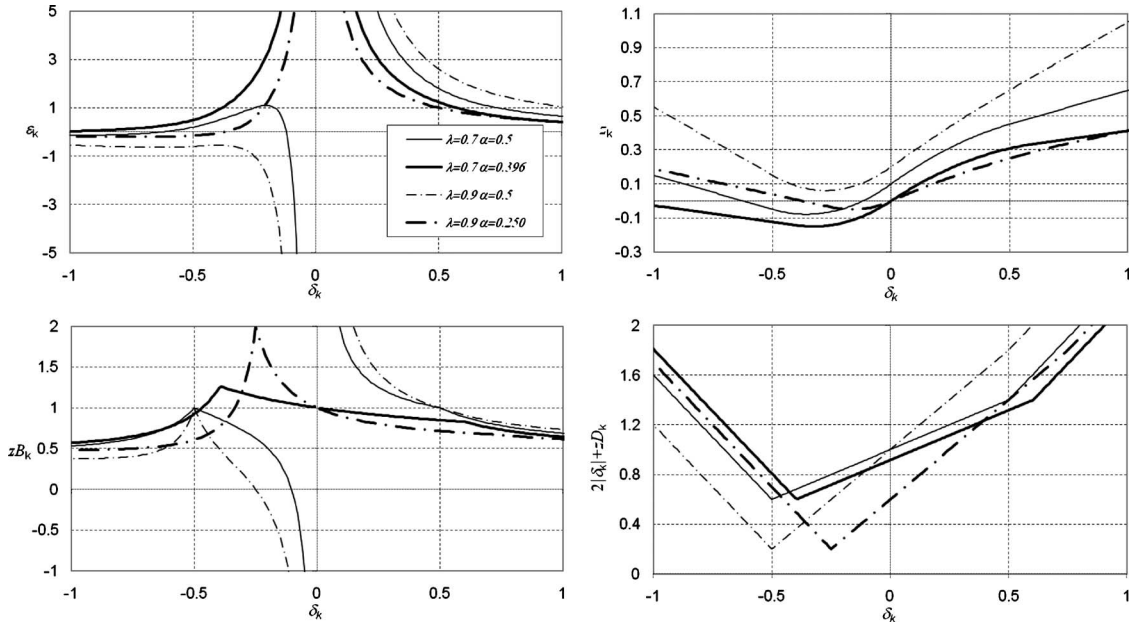

Fig. 4. Subplots of ε_k, z_k, zB_k, and variable part of $\mathbf{D}_{pp}$ as a function of δ_k ($m_k=1$, $\alpha=\alpha_k$, $\lambda=\lambda_{k,1}=\{0.7, 0.9\}$)

J. Hydraul. Eng., 2010, 136(11): 889-900

fact that there are configurations for negative Q_k (i.e., δ_k) for which the pipe head loss is overestimated. This is caused by $\alpha_k=0.5$, which is implicitly associated to an assumption of symmetric demand pattern and by the fact that the connection is placed in the second half of the pipe ($\lambda_{k,1}>0.5$). This condition is further clarified by the positive values of the subplot of z_k in Fig. 4 for $\delta_k<0$ which correspond to positive errors in energy balance for negative flows ($\delta_k<0$). In consequence, the assumption $\alpha_k=0.5$ is incorrect for nonsymmetric demand patterns and can cause a discontinuity and negative values of the correction factor ε_k. The subplot of zB_k (i.e., the diagonal elements of $\mathbf{B}_{pp}$ used in EGGA) in Fig. 4 further demonstrates the need for computing α_k because those values are no longer bounded as in Fig. 3.

Finally, the 4th subplot of Fig. 4 reports the curve $2|\delta_k|+zD_k$ whose values are the diagonal elements of $\mathbf{D}_{pp}$ used in EGGA [see Eqs. (11) and (12)] assumed $P_k=1$ and $R_{k,\infty}=1$. The fact that the values $2|\delta_k|+zD_k$ are always positive demonstrates that the correction zD_k becomes a sort of regularization term for $\mathbf{D}_{pp}$ for δ_k close to zero as will be better discussed in the section of numerical tests. It is a nice feature considering the convergence issue. Note that the minimum value of $2|\delta_k|+zD_k$ is always equal to $2(1-\lambda_{k,1})$.

It is worth noting that studying $\lambda_{k,1}=0.9$ is equivalent to $\lambda_{k,1}=0.1$ because those values, 0.9 or 0.1 and vice versa, are a consequence of the connection position with respect to the first node (i.e., positive flow direction). In fact, the problem is symmetrical with respect to the middle point of the pipe.

Strategy to Compute α_k for Nonsymmetric Patterns

The aim of this section is to study a strategy to compute α_k in order to obtain $\varepsilon_k>0$ also in the case of non symmetric demand patterns, thus avoiding the abovementioned numerical drawbacks. In the case of one connection in the position $\lambda_{k,1}=0.5$ (i.e., symmetric pattern), the "natural" assumption is $\alpha_k=0.5$ and produces $z_k=0$ for $\delta_k=0$ and $\varepsilon_k>0$ (see Fig. 3 case $m=1$). On the contrary, Fig. 4 shows that $z_k>0$ for $\delta_k=0$ assuming $\lambda_{k,1}=\{0.7,0.9\}$ (i.e., nonsymmetric demand patterns). This fact causes a positive correction ε_k for Q_k tending to zero from positive values and, vice versa, a negative correction ε_k for Q_k tending to zero from negative values (see top-left Fig. 4). Therefore, in order to correct the problem due to non symmetric demand patterns (which can generate convergence troubles in EGGA), the idea is to constrain z_k to zero for $\delta_k=0$ (i.e., $Q_k=0$) and to compute a coefficient α_k (different from 0.5) which is more liable for non symmetric patterns. Hence

$$z_k(\delta_k=0,m_k=1,\kappa_{k,1}=\kappa_{k,2})=\kappa_{k,1}\alpha_k|\alpha_k|^{n-1}\lambda_{k,1}+\kappa_{k,1}(\alpha_k-1)|\alpha_k-1|^{n-1}\lambda_{k,2}=\kappa_{k,1}\alpha_k^n\lambda_{k,1}-\kappa_{k,1}(1-\alpha_k)^n(1-\lambda_{k,1})=0\Rightarrow\alpha_k=[(\lambda_{k,1}/(1-\lambda_{k,1}))^{1/n}+1]^{-1}=[(\lambda_{k,1}/\lambda_{k,2})^{1/n}+1]^{-1} \quad (23)$$

where $\alpha_k>0$ and $\alpha_k-1<0$ has been considered to account for the absolute value, while $\lambda_{k,2}=1-\lambda_{k,1}$. The new curves ε_k and zB_k for $\lambda_{k,1}=\{0.7,0.9\}$ obtained by using the computed α_k (=0.396 and =0.250, respectively) are reported in the two related subplots of Fig. 4. They demonstrate that $\varepsilon_k>0$ and $zB_k>0$ close to $\delta_k=0$ have been achieved by computing α_k by Eq. (23). Furthermore, Fig. 4 evidences that $z_k(\delta_k=0)=0$ according to the assumption to obtain Eq. (23). The fact that z_k are positive and ε_k are slightly negative and tending to zero for $\delta_k<0$ when $\lambda_{k,1}=0.9$ does not cause negative values of zB_k or change the good property of EGGA with respect to $\mathbf{D}_{pp}$ inversion as clear from the two related subplots of Fig. 4. In addition, the subplot of $2|\delta_k|+zD_k$ in Fig. 4 shows that the computation of α_k only translates the curves whose minimum values is in $\delta_k=-\alpha_k$.

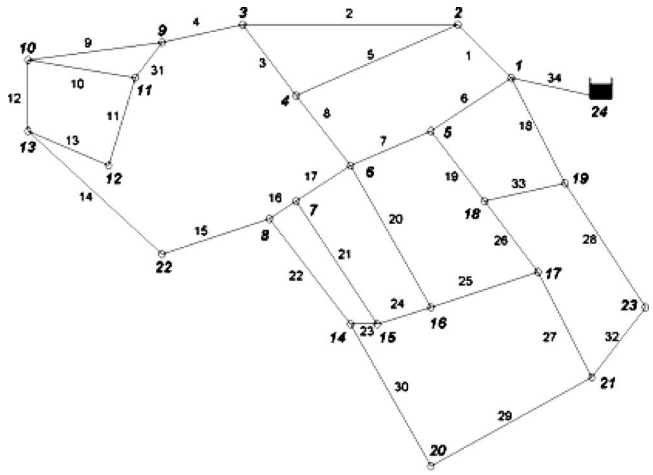

Fig. 5. Apulian network layout

Finally, the last issue is to compute α_k when $m_k>1$. Considering $q_{k,j}$, the center of mass criterion to compute a $\lambda_{k,1}=\lambda_{k,q}$, for Eq. (23), has been used here

$$\lambda_{k,q}=\sum_{j=1}^{m_k}\left(\frac{q_{k,j}}{P_k}\sum_{i=1}^{j}\frac{L_{k,i}}{L_k}\right)=\frac{1}{P_k}\sum_{j=1}^{m_k}\left(q_{k,j}\sum_{i=1}^{j}\lambda_{k,i}\right) \quad (24)$$

Case Study

The Apulian network depicted in Fig. 5 (for further details, see Giustolisi et al. 2008a or Giustolisi and Todini 2009) was used here for two purposes:

- To test EGGA from a numerical standpoint, by analysing convergence through some performance indicators and comparing EGGA with the classical GGA.
- To demonstrate that the hydraulic status can considerably change when the actual demand pattern is considered. To this purpose, the distribution throughout a randomly generated number of connections (m_k) uniformly spaced and delivering the same demand equal to P_k/m_k has been used.

Numerical Tests

The convergence tests have been performed considering

1. Randomly modified topology obtained by removing pipes in the network (Giustolisi et al. 2008a,b).
2. Random assignment of pipe diameters among those reported in Table 1. This is a powerful numerical test because the unitary hydraulic resistance $K_{k,\infty}$ for each pipe can vary in a very large range (i.e., from 0.247 to 265.14 $s^2\cdot m^{-6}$).
3. Darcy-Weisbach formulation of head losses without any assumption on flow regime.
4. Seven different demand patterns (see Table 2) using
   a. Uniform function (Giustolisi and Todini 2009).
   b. $\lambda_{k,i}=$const, $\pi_{k,i}=$const and a random number of connections (m_k) in the range [1 10]. α_k(=0.5) was not computed because of the symmetric demand pattern.

J. Hydraul. Eng., 2010, 136(11): 889-900

Table 1. Diameters and Unitary Hydraulic Resistances

D (m)	$K_{k,\infty}$ (s^2/m^6)
0.100	265.147
0.164	18.565
0.184	9.882
0.204	5.629
0.229	3.068
0.258	1.639
0.290	0.867
0.327	0.460
0.368	0.247

c. $\lambda_{k,i}$=const, $\pi_{k,i}$=const and m_k=10, α_k(=0.5) was not computed because of the symmetric demand pattern.
d. $\lambda_{k,i}$=const, random $\pi_{k,i}$ (uniformly distributed in the range [0 1]) with m_k=10 and α_k=0.5.
e. $\lambda_{k,i}$=const, random $\pi_{k,i}$ (uniformly distributed in the range [0 1]) with m_k=10, and α_k computed as in Eq. (23).
f. Random $\lambda_{k,1}$ (uniformly distributed in the range [0 1]) with m_k=1 and α_k=0.5.
g. Random $\lambda_{k,1}$ (uniformly distributed in the range [0 1]) with m_k=1 and α_k computed as in Eq. (23).

Table 2 reports, for each of seven demand patterns (EGGA) and for the classical GGA, the statistics of the 10,000 simulations considering both the maximum energy/mass balance errors (1st and 2nd columns), and the average and maximum number of iterations (3rd and 4th columns). The statistics reported in Table 2 are computed assuming the mean of squared errors equal to 10^{-7} as stopping criterion for convergence reaching. Furthermore, the following linear solution with respect to Q_k was always adopted in order to initialize Q_k both in EGGA and GGA:

$$\mathbf{F}_n = \mathbf{d}_n + \mathbf{A}_{np}(\mathbf{D}_{pp})^{-1}(\mathbf{A}_{p0}\mathbf{H}_0)$$

$$\mathbf{H}_n = -(\mathbf{A}_{np}(\mathbf{D}_{pp})^{-1}\mathbf{A}_{pn})^{-1}\mathbf{F}_n$$

$$\mathbf{Q}_p^1 = -(\mathbf{D}_{pp})^{-1}(\mathbf{A}_{p0}\mathbf{H}_0 + \mathbf{A}_{pn}\mathbf{H}) \tag{25}$$

where the elements of the diagonal matrix $\mathbf{D}_{pp}$=pipe hydraulic resistances $R_{k,\infty}$. This initialization was found to be best compared to other alternatives. The results in Table 2 demonstrate that:

1. Convergence of EGGA is faster than GGA as shown by the average and maximum numbers of iterations (i.e., the number of iterative solutions of the system of linear equations, thus the algorithm initialization has been comprised) among the 10,000 simulations which decreases from 5.20 to about 4.5 and from 13 to about 6, respectively;
2. EGGA is more robust GGA. In fact, 0.47% of times the over-relaxation parameter was used (see for further details Giustolisi et al. 2008a) in order to reach the convergence in GGA, compared with the 0% for EGGA; and
3. The computation of α_k is useful for EGGA convergence and robustness. In fact, comparing the 6th and 7th demand patterns, the average number of iterations decreases from 5.11 to 4.47 and the maximum number of iterations from 101 to 7. Furthermore, the simulation using the 6th demand pattern and α_k=0.5 required the overrelaxation parameter 1% of times which was never used in the other case (7th demand pattern).

To explain the different convergence properties of EGGA with respect to GGA, it is necessary to report that they differ from each other in the following:

1. The matrix $\mathbf{D}_{pp}$ whose elements are $n|Q_k|^{n-1}R_{k,\infty}$ and $(n|Q_k|^{n-1}+zD_kP_k^{n-1})R_{k,\infty}$, respectively and
2. The matrix $\mathbf{B}_{pp}$ whose elements are constant in GGA [equal to $1/n$, see Eq. (11) for $zA_k=zD_k=0$] and variable in EGGA.

The superiority of EGGA convergence properties with respect to GGA is due to the term $zD_kP_k^{n-1}$ which is an added term to diagonal of $\mathbf{D}_{pp}$. In fact, system (10) (formally similar to GGA and EGGA) requires the inversion of $\mathbf{D}_{pp}$ which is automatically regularized in EGGA strategy (i.e., when $P_k>0$ because for $P_k=0$ EGGA and GGA coincide). In order to prove this fact, the general correction zD_k (due to minor head losses and demand patterns) needs to be analysed

$$zD_k = -n|\delta_k|^{n-1} + \sum_{i=0}^{m_k}\left(P_k\frac{d\kappa_{k,i+1}}{dQ_{k,i+1}}(\delta_k+\alpha_k-\pi_{k,i}) + n\kappa_{k,i+1}\right)|\delta_k+\alpha_k - \pi_{k,i}|^{n-1}\lambda_{k,i+1} + 2\frac{A_{k,1}^2}{A_{k,i}^2}K_{k,i}^{ml}G_k|\delta_k+\alpha_k-\pi_{k,i}| \tag{26}$$

Assuming Q_k=0 both in GGA and in EGGA (i.e., δ_k=0)

$$zD_k = \sum_{i=0}^{m_k}\left(P_k\frac{d\kappa_{k,i+1}}{dQ_{k,i+1}}(\alpha_k-\pi_{k,i}) + n\kappa_{k,i+1}\right)|\alpha_k-\pi_{k,i}|^{n-1}\lambda_{k,i+1} + 2\frac{A_{k,1}^2}{A_{k,i}^2}K_{k,i}^{ml}G_k|\alpha_k-\pi_{k,i}| > 0 \Rightarrow D_{pp}^{\mathrm{EGGA}}(k,k) = R_{k,\infty}zD_kP_k^{n-1} > 0$$

Table 2. Convergence Statistics of GGA versus EGGA

Demand patterns		Among the 10,000 simulations: Maximum energy balance error (m)	Maximum mass balance error (m^3/s)	Average number of iterations	Maximum number of iterations
Classical GGA		2.368×10^{-3}	1.49×10^{-9}	5.20	13
EGGA	Uniform function	2.328×10^{-3}	5.63×10^{-11}	4.51	6
	$\pi_{k,i}$=const and random m_k in [1,10]	2.363×10^{-3}	1.19×10^{-11}	4.43	6
	$\pi_{k,i}$=const and m_k=10	2.328×10^{-3}	2.1×10^{-11}	4.48	6
	Random $\pi_{k,i}$, m_k=10, α_k=0.5	2.37×10^{-3}	3.75×10^{-11}	4.47	6
	Random $\pi_{k,i}$, m_k=10, α_k computed	2.335×10^{-3}	3.01×10^{-11}	4.47	6
	Random $\lambda_{k,1}$, m_k=1, α_k=0.5	2.379×10^{-3}	3.3×10^{-10}	5.11	101
	Random $\lambda_{k,1}$, m_k=1, α_k computed	2.364×10^{-3}	6.26×10^{-10}	4.47	7

J. Hydraul. Eng., 2010, 136(11): 889-900

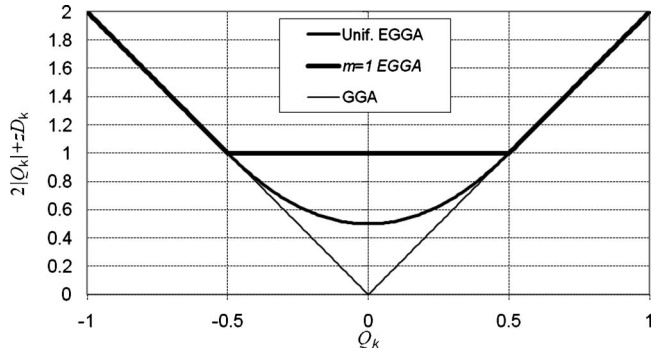

Fig. 6. Graphical representation of variable part of $\mathbf{D}_{pp}$

$$D_{pp}^{\mathrm{GGA}}(k,k) = 0 \tag{27}$$

Thus, $\mathbf{D}_{pp}$ becomes not invertible if any kth pipe has model flow (Q_k) equal to zero in GGA, while $\mathbf{D}_{pp}$ is always invertible in the same conditions in EGGA. This fact is also graphically evidenced by the subplot of the variable part of $\mathbf{D}_{pp}$, $(2|Q_k|+zD_k)$, in Fig. 4 where $P_k=R_{k,\infty}=1$ and $n=2$ has been assumed and in Fig. 6 where the same variable has been plotted for EGGA (uniform function and one connection in the middle of the pipe) and for GGA. The inversion of $\mathbf{D}_{pp}$ becomes ill-conditioned in GGA approaching Q_k to zero, this fact results into convergence problems. On the contrary, Figs. 4 and 6 further prove that $\mathbf{D}_{pp}$ is always invertible in EGGA strategy. The need for regularization of $\mathbf{D}_{pp}$ in GGA was already addressed in Carpentier et al. (1987) and in Piller (1995) which presented and proved a Tikhonov regularisation strategy (Tikhonov 1963). Their findings (see in particular the graphical representation of $\mathbf{D}_{pp}$ in Piller 1995, p. 89) fully confirm the convergence features of EGGA strategy. Furthermore, Eq. (27) demonstrates that the implicit regularization properties of EGGA still hold considering large values of minor head losses which in turn can generate very low values of Q_k (i.e., δ_k). In addition, for $zD_k<0$, the case of nonsymmetric demand patterns, α_k is computed by Eq. (23) and $|zD_k|<2|\delta_k|$ holds, as shown in Fig. 4.

Considering $\mathbf{B}_{pp}$ and the last equation of system (10), the term $(\mathbf{I}_{pp}-\mathbf{B}_{pp})$ could be a source of convergence troubles as demonstrated by the case on non-symmetric demand pattern where the over-relaxation parameter was used 1% of time and the maximum number iteration was equal to 101. Consequently, the computation of α_k by Eq. (23) for nonsymmetric demand patterns is helpful because it bounds zB_k, see the related subplot in Fig. 4, although the overrelaxation parameter remains beneficial in the cases characterized by $zB_k>2$ for few pipes where inversion of flow occurs and, contemporarily, the only one active connection is very close to one of the terminal node.

Network Hydraulic Status: GGA versus EGGA

The network in Fig. 5 with a randomly generated number of connections (m_k), see second column of Table 3, has been used here in order to demonstrate that EGGA and GGA could provide different hydraulic results due to energy balance correction need of Eq. (7) which is dependent on the absolute value of total pipe-level demand P_k, see third column of Table 3. Connections are assumed to be uniformly spaced and delivering the same demand (equal to P_k/m_k). The number of connections of Pipe 34 is always zero because it does not distribute any water. Then, the hydraulic status of the network in Fig. 5 (i.e., pipe discharges $\mathbf{Q}_p$ and nodal heads $\mathbf{H}_n$) have been computed using GGA and EGGA. $\alpha_k=0.5$ has been assumed in both cases (i.e., GGA and EGGA) being the demand patterns symmetric. Therefore, the definition of the pipe hydraulic resistance is the key difference between the two approaches: $R_{k,\infty}$ and $R_{k,\infty}(1+\varepsilon_k)$ for GGA and EGGA, respectively. As reported in Table 3, it results to a different flow distribution (see columns $\mathbf{Q}_{\mathrm{GGA}}$ and $\mathbf{Q}_{\mathrm{EGGA}}$) and, consequently, to different pipe head losses (see columns $\mathbf{E}_{\mathrm{GGA}}$ and $\mathbf{E}_{\mathrm{EGGA}}$). The pipe head loss difference descends from the pipe hydraulic resistance correction (ε_k) which, in turn, depends on the number of connections (m_k) and on the ratio between the flow (Q_k) and the distributed demand (P_k). Consequently, the above differences of pipe head losses result to different nodal heads and pressures between GGA and EGGA. The results reported in Table 3 show that:

- Pressure in Node 1 does not change with demand pattern because Pipe 34 does not distribute any water and the network total demand (=0.2821 m^3/s) is unchanged.
- Pipe head losses in EGGA (i.e., when the pipe demand pattern is considered) are generally greater than in GGA (see columns $\mathbf{E}_{\mathrm{GGA}}$ and $\mathbf{E}_{\mathrm{EGGA}}$ of Table 3). This is due to ε_k which is always a positive correction (see 4th column of Table 3). The flows computed by GGA and EGGA are different but do not justify the head loss increase in EGGA (see columns $\mathbf{Q}_{\mathrm{GGA}}$ and $\mathbf{Q}_{\mathrm{EGGA}}$).
- Nodal pressures (i.e., nodal heads) computed by EGGA are generally lower (see columns $\mathbf{P}_{\mathrm{GGA}}$ and $\mathbf{P}_{\mathrm{EGGA}}$ of Table 3). This is a direct consequence of the general underestimation of pipe head losses of GGA with respect to EGGA.
- Percentage of pressure difference, $100\cdot(\mathbf{P}_{\mathrm{EGGA}}-\mathbf{P}_{\mathrm{GGA}})/\mathbf{P}_{\mathrm{GGA}}$, reported in the last columns of Table 3 demonstrates that pressure status could significantly change. In fact, there are some nodes whose absolute value of pressure difference is greater than 15%. Furthermore, the Nodes 12, 13, and 23 become critical being the pressure value significantly less than 10 m. This is an important point considering the common use of classical GGA for network design purposes.

Finally, a consideration about the general network functioning predicted by EGGA (i.e., accounting for pipe demand patterns) with respect to GGA (i.e., not accounting for pipe demand patterns) needs to be provided. Fig. 5, together with Table 3 (in particular the last column and columns of $\mathbf{E}_{\mathrm{GGA}}$ and $\mathbf{E}_{\mathrm{EGGA}}$) show that the hydraulic status of the path connecting Nodes 1, 5, 6, 7, 8, and 22 results were not considerably changed by the use of EGGA. Indeed, it is a principal flow path of the network because its main task is to transfer the water in other parts of the network from water source (Node 24). Thus, Pipes 6, 7, 15, 16, and 17 of the principal flow path are characterized by a large value of δ_k (i.e., the ratio between Q_k, transferred water, and P_k, distributed water). Thus, the corresponding pipe hydraulic resistance correction ε_k is low as in Table 3. On the other hand, some nodes (e.g., 4, 12, 13, 14, 15, 16, 17, 21, and 23) belonging to "secondary" flow paths are characterized by pipes with a generally low δ_k [i.e., amount of transferred water (Q_k) is low with respect to distributed one (P_k)]. For this reason, those nodes are more sensitive to a correct simulation of the network behavior because the way P_k is distributed becomes more important.

Once again, it is important to emphasize that increasing δ_k EGGA tends to coincide with GGA, from the hydraulic and technical point of view. In fact, decreasing P_k and $R_{k,\infty}$ [see Eq. (7)] EGGA nodal heads become similar to that provided by classical GGA, whilst EGGA numerical and computational features still hold. This means that even if the energy balance correction induced by EGGA is negligible (although this is difficult to dem-

J. Hydraul. Eng., 2010, 136(11): 889-900

Table 3. Hydraulic Status: GGA versus EGGA

Pipe id	m_k	P_k (m^3/s)	ε_k	$\mathbf{Q}_{GGA}$ (m^3/s)	$\mathbf{Q}_{EGGA}$ (m^3/s)	$\mathbf{E}_{GGA}$ (m)	$\mathbf{E}_{EGGA}$ (m)	Node id	$\mathbf{P}_{GGA}$ (m)	$\mathbf{P}_{EGGA}$ (m)	Pressure difference (%)
1	3	0.0057	0.0005	0.0962	0.097	1.48	1.51	1	26.90	26.90	0
2	1	0.0155	0.0105	0.0737	0.0758	4.5	4.81	2	24.81	24.78	−0.12
3	8	0.0078	0.3447	0.0036	0.0043	1.68	3.17	3	21.30	20.97	−1.55
4	7	0.0065	0.0014	0.0552	0.0566	1.06	1.11	4	17.22	15.41	−10.51
5	3	0.0129	1.1761	0.0054	0.0042	6.18	7.98	5	23.54	23.54	0
6	9	0.0066	0.0002	0.1538	0.1538	2.36	2.36	6	20.10	20.17	0.35
7	5	0.0063	0.0005	0.1012	0.0992	1.84	1.77	7	18.91	19.01	0.53
8	3	0.0078	0.2526	0.0052	0.0058	3.46	5.36	8	17.90	18.01	0.61
9	4	0.0152	4.4945	0.0035	0.0017	3.09	4.04	9	17.85	17.46	−2.18
10	1	0.0070	0.0149	0.025	0.0286	2.67	3.55	10	12.66	11.32	−10.58
11	1	0.0083	0.675	0.0054	0.0051	4	5.81	11	16.23	15.77	−2.83
12	6	0.0070	0.0219	0.014	0.0158	0.83	1.08	12	10.12	7.86	−22.33
13	10	0.0068	0.7155	−0.0021	−0.0025	0.5	1.19	13	10.03	8.44	−15.85
14	7	0.0166	3.9424	0.0034	0.0019	3.06	5.01	14	15.41	15.44	0.19
15	1	0.0074	0.0705	0.0154	0.0139	1.99	1.76	15	14.00	13.00	−7.14
16	8	0.0030	0.0002	0.062	0.0614	0.61	0.6	16	14.36	13.06	−9.05
17	2	0.0036	0.0004	0.0757	0.0742	1.1	1.06	17	15.30	14.62	−4.44
18	1	0.0095	0.0542	0.0212	0.0204	4.86	4.76	18	18.83	18.59	−1.27
19	5	0.0073	0.0031	0.0426	0.0445	2.52	2.75	19	19.35	19.44	0.47
20	9	0.0129	0.9807	0.005	0.004	5.25	6.6	20	10.01	9.98	−0.3
21	8	0.0117	0.9837	0.0045	0.0036	3.92	5.01	21	11.48	9.96	−13.24
22	4	0.0107	0.0105	0.0361	0.0369	1.4	1.48	22	14.00	14.36	2.57
23	1	0.0027	0.028	−0.0066	−0.0081	1.91	2.94	23	10.45	6.87	−34.26
24	5	0.0041	0.3237	−0.0019	−0.0025	0.24	0.54	24	H_0=21.4+15	H_0=21.4+15	0
25	9	0.0054	0.131	0.0043	0.0048	1.64	2.25				
26	8	0.0081	0.0057	0.0323	0.0345	2.93	3.37				
27	2	0.0094	0.044	0.0165	0.0183	2.93	3.76				
28	2	0.0137	1.2135	0.006	0.0049	8.03	11.67				
29	10	0.0129	2.8992	−0.0025	−0.0019	1.33	2.82				
30	3	0.0138	0.1144	−0.0159	−0.0152	2.1	2.16				
31	3	0.0027	0.0006	0.0395	0.0427	0.42	0.49				
32	3	0.0070	0.2256	−0.0044	−0.0055	2.15	4.19				
33	3	0.0062	3.8954	0.0005	0.0008	0.02	0.35				
34	0	0	0	0.2821	0.2821	3.1	3.1				

onstrate a priori or using GGA itself), EGGA remains a method to reduce the dimension of the topological representation of the hydraulic network for simulation purposes.

Conclusions

An extension of the GGA (EGGA) allowing the effective introduction of the lumped nodal demands without forfeiting the correct pipe head loss has been presented. A pipe hydraulic resistance correction (Giustolisi and Todini 2009) has been used in order to modify the classical GGA. The formulation of the pipe hydraulic resistance correction for any pipe demand pattern due to pipe connections has been achieved. Consequently, some dimensionless correction factors have been formulated to account for any pipe demand pattern, valves and pumps. EGGA has been proven to be more convergent than GGA. Furthermore, it has been demonstrated that the network hydraulic status could considerably change using EGGA depending on total demand distributed along pipes. EGGA can be easily implemented in all simulation packages based on GGA, such as in EPANET 2, and it can serve as a guide for other network simulation model strategies. Furthermore, it is envisaged that the new simulation model is essential for network model calibration purposes and also for other network analyses such as pressure-driven leakage and demand simulation model (Giustolisi et al. 2008c).

Appendix. Formulation of Total Pipe Head Loss Corrections

The formulation for total pipe head loss corrections is reported here for the case $n=2$ and $R_k=$const, corresponding to Darcy-Weisbach relationship for fully rough turbulent flow (Giustolisi and Todini 2009). Actually, they were originally written for $|\delta_k| = |Q_k|/P_k$, while they are reported here using δ_k. Hence

$$\varepsilon_k = \begin{cases} \dfrac{\frac{2}{3}|\delta_k|^3 - \delta_k^2 + \frac{1}{2}|\delta_k|}{\delta_k^2} & -\dfrac{1}{2} < \delta_k < \dfrac{1}{2} \\ \dfrac{1}{12\delta_k^2} & \delta_k \le -\dfrac{1}{2}, \delta_k \ge \dfrac{1}{2} \end{cases}$$

$$z_k = \begin{cases} \left(\frac{2}{3}|\delta_k|^3 - \delta_k^2 + \frac{1}{2}|\delta_k|\right)\text{sign}(\delta_k) & -\frac{1}{2} < \delta_k < \frac{1}{2} \\ \frac{1}{12}\text{sign}(\delta_k) & \delta_k \le -\frac{1}{2}, \delta_k \ge \frac{1}{2} \end{cases}$$

$$zA_k = \begin{cases} \frac{2}{3}\delta_k^2 - |\delta_k| + \frac{1}{2} & -\frac{1}{2} < \delta_k < \frac{1}{2} \\ \frac{1}{12|\delta_k|} & \delta_k \le -\frac{1}{2}, \delta_k \ge \frac{1}{2} \end{cases}$$

$$zD_k = \begin{cases} 2\delta_k^2 - 2|\delta_k| + \frac{1}{2} & -\frac{1}{2} < \delta_k < \frac{1}{2} \\ 0 & \delta_k \le -\frac{1}{2}, \delta_k \ge \frac{1}{2} \end{cases}$$

$$zB_k = \begin{cases} \frac{4\delta_k^2 + 3}{12\delta_k^2 + 3} & -\frac{1}{2} < \delta_k < \frac{1}{2} \\ \frac{1}{2}\left(1 + \frac{1}{12\delta_k^2}\right) & \delta_k \le -\frac{1}{2}, \delta_k \ge \frac{1}{2} \end{cases} \quad (28)$$

Notation

The following symbols are used in this paper:

$A_{k,i}$ = internal cross sectional area of ith inline trunk of kth pipe;
$\mathbf{A}_{np}$ = topological incidence submatrix of WDN model;
$\mathbf{A}_{pp}$ = diagonal matrix of WDN model;
$\mathbf{A}_{p0}$ = topological incidence submatrix of WDN model;
$\bar{\mathbf{A}}_{pn}$ = general topological submatrix of WDN model;
$\mathbf{B}_{pp}$ = diagonal matrix used in GGA and EGGA;
D_k = internal diameter of kth pipe;
$D_{k,i}$ = internal diameter of ith inline trunk of kth pipe;
$\mathbf{D}_{pp}$ = diagonal matrix used in GGA and EGGA;
$\mathbf{d}_n$ = vector of nodal demands of WDN model;
E_k = head loss of kth pipe;
$\mathbf{E}_{\text{EGGA}}$ = vector of pipe head losses using EGGA;
$\mathbf{E}_{\text{GGA}}$ = vector of pipe head losses using GGA;
$\mathbf{F}_n$ = temporary matrix used in GGA and EGGA;
f_k = friction factor of kth pipe;
$f_{k,\infty}$ = friction factor of fully rough turbulent flow of first inline trunk;
G_k = parameter useful in correction factors accounting for minor head losses;
g = gravitational acceleration;
H_A, H_B = nodal heads (in A and B) of system;
$\mathbf{H}_n$ = vector of total network heads of WDN model;
$\mathbf{H}_0$ = vector of total fixed (i.e., known) network heads of WDN model;
$\mathbf{I}_{pp}$ = identity matrix;
i, j = index of inline trunks and nodes, respectively;
iter = counter of GGA or EGGA solver;
$K_{k,i}$ = unitary pipe hydraulic resistance of ith inline trunk of kth pipe;
$K_{k,\infty}$ = unitary hydraulic resistance of fully rough turbulent flow of first inline trunk;
$K_{k,i}^{ml}$ = minor head loss coefficient of ith inline trunk of kth pipe;
Ke = equivalent roughness;
k = index of pipes;
L_k = total length of the kth pipe;
$L_{k,i}$ = length of ith inline trunk of kth pipe;
m_k = number of connections of kth pipe;
n = head loss equation exponent;
n_n = total number of network internal nodes;
n_p = total number of network pipes;
n_0 = total number of known heads;
on = Boolean variable accounting for pump installation direction;
P_k = total distributed demand along kth pipe;
$\mathbf{P}_{\text{EGGA}}$ = vector of nodal pressures using EGGA;
$\mathbf{P}_{\text{GGA}}$ = vector of nodal pressures using GGA;
$\mathbf{P}_p$ = pipe demand vector whose elements P_k;
Q_k = discharge of kth pipe in WDN model;
$Q_{k,i}$ = discharge of ith inline trunk of kth pipe;
$\mathbf{Q}_p$ = vector of pipe flows/discharges in WDN model;
$\mathbf{Q}_{\text{EGGA}}$ = vector of pipe flows using EGGA;
$\mathbf{Q}_{\text{GGA}}$ = vector of pipe flows using GGA;
$q_{k,j}$ = demand at jth inline node of kth pipe;
Re = Reynolds number;
$R_{k,\infty}$ = pipe hydraulic resistance of fully rough turbulent flow;
$\mathbf{R}_p$ = vector of pipe resistances;
sign() = variable sign operator;
z_k, zA_k, zD_k, zB_k = dimensionless correction factors of EGGA of kth pipe;
α_k = coefficients used for concentrating pipe demand of kth pipe;
δ_k = ratio between Q_k and P_k;
ε_k = hydraulic resistance correction factor of kth pipe;
$\kappa_{k,i}$ = ratio between $K_{k,i}$ and $K_{k,\infty}$;
$\mathbf{\Lambda}_{np}$ = matrix of α_k and $(1-\alpha_k)$ to generate lumped nodal demands;
$\lambda_{k,i}$ = ratio between $L_{k,i}$ and L_k;
$\lambda_{k,q}$ = center of mass of demand pattern of kth pipe;
$\pi_{k,i}$ = ratio between $\Sigma_j(q_{k,j})$ and P_k;
$\omega_{k,p}$, $H_{k,p}$, $r_{k,p}$, γ = speed factor and parameters of pump curve of kth pipe;
$(\,)^T$ = vector/matrix transpose operator; and
$(\,)^{-1}$ = matrix inverse operator.

References

Anderson, E. J., and Al-Jamal, K. H. (1995). "Hydraulic network simplification." *J. Water Resour. Plann. Manage.*, 121(3), 235–240.

Carpentier, P., Cohen, G., and Hamam, Y. (1987). "Water network equilibrium variational formulation and comparison of numerical algorithms." *Computer application in water supply*, Vol. 1, Wiley, New York.

Collins, M., Cooper, L., Helgason, R., Kenningston, J., and LeBlanc, L. (1978). "Solving the pipe network analysis problem using optimization techniques." *Manage. Sci.*, 24(7), 747–760.

Cross, H. (1936). "Analysis of flow in networks of conduits or conductors." *Bulletin no. 286*, Univ. of Illinois Engineering Experimental Station, Urbana, Ill., 1–29.

Epp, R., and Fowler, A. G. (1970). "Efficient code for steady-state flows in networks." *J. Hydr. Div.*, 96(11), 3–56.

Giustolisi, O., Kapelan, Z., and Savic, D. A. (2008a). "An algorithm for automatic detection of topological changes in water distribution networks." *J. Hydraul. Eng.*, 134(4), 435–446.

Giustolisi, O., Kapelan, Z., and Savic, D. A. (2008b). "Detecting topological changes in large water distribution networks." *Proc. Water Distribution Systems Analysis (WDSA)*, ASCE, Reston, Va., 865–872.

Giustolisi, O., Savic, D. A., and Kapelan, Z. (2008c). "Pressure-driven demand and leakage simulation for water distribution networks." *J. Hydraul. Eng.*, 134(5), 626–635.

Giustolisi, O., and Todini, E. (2009). "Pipe hydraulic resistance correction in WDN analysis." *Urban Water*, 6(1), 39–52.

Hamam, Y. M., and Brammeler, A. (1971) "Hybrid method for the solution of piping networks." *Proc. IEEE*, 118(11), 1607–1612.

Hamberg, D., and Shamir, U. (1988). "Schematic models for distribution systems design: I. Combination concept." *J. Water Resour. Plann. Manage.*, 114(2), 129–140.

Isaacs, L. T., and Mills, K. G. (1980). "Linear theory method for pipe network analysis." *J. Hydr. Div.*, 106(7), 1191–2001.

Kesavan, H. K., and Chandrashekar, M. (1972). "Graph-theoretic models for pipe network analysis." *J. Hydr. Div.*, 98(2), 345–364.

Martin, D. W., and Peters, G. (1963). "The application of Newton's method to network analysis by digital computers." *J. Inst. Water Eng.*, 17, 115–129.

Osiadacz, A. J. (1987). *Simulation and analysis of gas networks*, E & FN Spon, London.

Piller, O. (1995). "Modeling the behavior of a network—Hydraulic analysis and a sampling procedure for estimating the parameters." Ph.D. thesis, Univ. of Bordeaux I, Bordeaux, France.

Rossman, L. A. (2000). *EPANET 2 user's manual*, U.S. EPA, Cincinnati.

Shamir, U., and Howard, C. D. D. (1968). "Water distribution network analysis." *J. Hydr. Div.*, 94(1), 219–234.

Tikhonov, A. N. (1963). "Solution of incorrectly formulated problems and the regularization method." *Dokl. Akad. Nauk SSSR*, 151, 501–504.

Todini, E. (1979). "Un metodo del gradiente per la verifica delle reti idrauliche (A gradient method for the solution of hydraulic networks)." *Bollettino degli Ingegneri della Toscana*, 11, 11–14 (in Italian).

Todini, E., and Pilati, S. (1988). "A gradient method for the solution of looped pipe networks." *Proc., Computer Applications in Water Supply*, Vol. 1, Wiley, New York, 1–20.

Ulanicki, B., Zehnpfund, A., and Martínez, F. (1996). "Simplification of water distribution network models." *Proc., Hydroinformatics '96*, Balkema, Rotterdam, 493–500.

Wood, D. J., and Charles, C. O. A. (1972). "Hydraulic network analysis using linear theory." *J. Hydr. Div.*, 98(7), 1157–1170.

Wood, D. J., and Rayes, A. G. (1981). "Reliability of algorithms for pipe network analysis." *J. Hydr. Div.*, 107(10), 1145–1161.